J Ther Eng, Vol. 11, No. 2, pp. 331−343, March, 2025

Journal of Thermal Engineering
Web page info: https://jten.yildiz.edu.tr
DOI: 10.14744/thermal.0000898

Research Article

# Experimental investigation of convective heat transfer performance using sporadic flow divider type inserts

**Suryaji S. KALE[1,*], Sanjaykumar S. GAWADE[2]**

[1]*Department of Technology (Mechanical Engineering), Shivaji University, Maharashtra, 416004, India*
[2]*Department of Mechanical Engineering, K. E. Society's Rajarambapu Institute of Technology, Rajaramnagar - Affiliated to Shivaji University, Maharashtra, 415414, India*

## ARTICLE INFO

*Article history*
Received: 04 April 2024
Revised: 01 September 2024
Accepted: 03 October 2024

**Keywords:**
Flow Divider Type; Heat Transfer Enhancement; Inserts; Reynolds Number

## ABSTRACT

The depletion of conventional energy resources highlights the growing need for efficient utilization of available energy sources. Heat exchangers play a vital role in transferring heat between two or more fluids, and enhancing their performance is crucial for improving energy efficiency. Various techniques, categorized as active, passive, or hybrid methods, can be employed to augment heat transfer in heat exchangers. This experimental study investigates the use of innovative sporadic flow divider inserts as a passive method for heat transfer enhancement. The experiments were conducted using inserts with different twist angles of 90°, 60°, 45°, and 30°, over a range of Reynolds numbers from 7000 to 21000. The effect of spacing between the inserts was also analyzed using different space ratios (0.19, 0.39, 0.59, 0.78) in combination with the various twist angles.

The results indicated that higher Reynolds numbers led to increased Nusselt numbers, a decrease in the Thermal Enhancement Factor ($\psi$), and a reduction in the Friction Factor ($f$). Among the tested configurations, the 45° twist angle insert exhibited the highest Thermal Enhancement Factor ($\psi$) and Overall Performance Criteria ($\eta$) across most conditions. Conversely, the 30° twist angle resulted in a significantly higher friction factor, impeding fluid flow. The optimal performance was achieved with a 45° twist angle and a space ratio of 0.59, yielding a 23% improvement in Thermal Enhancement Factor ($\psi$) and a 55% increase in Overall Performance Criteria ($\eta$) compared to a plain tube. These findings demonstrate that sporadic flow divider inserts can effectively enhance convective heat transfer with a moderate increase in friction, ultimately improving the Overall Performance Criteria ($\eta$).

**Cite this article as:** Kale SS, Gawade SS. Experimental investigation of convective heat transfer performance using sporadic flow divider type inserts. J Ther Eng 2025;11(2):331−343.

***Corresponding author.**
*E-mail address: kalesss@gmail.com

*This paper was recommended for publication in revised form by Editor-in-Chief Ahmet Selim Dalkılıç*

## INTRODUCTION

Convective heat transfer holds notable importance in diverse engineering applications, influencing the efficacy of heat exchangers, cooling systems, and thermal management devices. The present research focuses on the exploration and enhancement of convective heat transfer by strategically incorporating flow divider inserts.

Flow dividers, integral components in fluidic systems, have the potential to bring about substantial changes in flow patterns and heat transfer characteristics. The thoughtful integration of these inserts enables the manipulation of fluid dynamics, fostering improved convective heat transfer. This paper presents a comprehensive investigation into the effects, mechanisms, and optimization strategies associated with integrating flow divider inserts to enhance convective heat transfer.

Through extensive experimentation, this study aims to provide valuable insights into the thermal performance enhancements achievable through the strategic use of flow dividers. The research considers various parameters, including geometric configurations, flow rates, and operational conditions, to unravel the intricate interplay between flow dividers and convective heat transfer. The objective of the study is to investigate experimentally, forced convection heat transfer and pressure drop characteristics with sporadic introduction of bisectional passive inserts.

The findings of this study not only deepen the understanding of convective heat transfer enhancement but also offer practical implications for the design and optimization of heat exchange systems in diverse engineering sectors. This comprehensive exploration highlights the potential advantages of integrating flow divider inserts for improved convective heat transfer, paving the way for more efficient and sustainable thermal management solutions.

The persistent pursuit of enhancing convective heat transfer has been a longstanding focus in thermal engineering. Researchers have explored various techniques to improve the efficiency of heat exchange systems. Among the innovative approaches gaining attention is the strategic implementation of flow divider inserts, introducing alterations in fluid dynamics to optimize convective heat transfer. Literature available in the field examines key studies contributing to the understanding of convective heat transfer enhancement, laying the groundwork for the current comprehensive investigation. Kumar and Jhinge [1] conducted experiments on a Shell-and-Tube Heat Exchanger (STHE) employing segmental baffles at various locations and with varying Reynolds numbers. Bichkar et al. [2] performed numerical simulations with different types of baffles, focusing on the impact of pressure drop in the STHE. They demonstrated that the use of helical baffles led to an improvement in thermal efficiency. Ali et al. [3] investigated the influence of tube length and shell diameter on pressure drop (ΔP) and Heat Transfer Coefficient (HTC) for the shell side, considering triangular and square pitch arrangements. Their findings indicated an increase in HTC with reduced cutting space and baffle spacing. Joemer et al. [4] utilized Computational Fluid Dynamics (CFD) software to optimize the baffle cut and angle in the STHE. Son and Shin [5] explored heat exchangers utilizing spiral baffle plates, emphasizing the rational fluid contact with the inner shell. Petrik and Szepesi [6] statistically studied shell-and-tube exchangers with horizontal baffles, comparing their results with the commercial program SC – Tetra V11.

Edward and Volker [7] investigated the influence of pressure drop, particularly on the shell side, in heat exchangers with segmental baffles. They used correlations for pressure drop calculations in an ideal tube bank and applied correction factors to account for leakage and bypass streams. Their study identified ranges of geometric and operational parameters where the experimental and theoretical results differed by no more than ± 35%. Gu et al. [8] performed experimental and numerical analyses on a trapezoidal baffled heat exchanger to evaluate the heat transfer coefficient, flow resistance, and overall thermal performance on the shell side. They found that compared to a shutter baffle heat exchanger, a twisty flow heat exchanger can enhance the heat transfer coefficient by 7.3–10.2%, decrease the pressure drop by 18.5–21%, and improve the thermal performance factor (TEF) by 14.9–19.2%. Akpabio et al. [9] studied the effect of baffle spacing on the overall heat transfer coefficient in a heat exchanger with a fixed baffle cut. Their research indicated that the optimal overall heat transfer coefficients in shell-and-tube heat exchangers are generally achieved with a baffle cut of 20 to 25 percent of the diameter. The maximum baffle spacing is determined by the tube support requirements. Singh et al. [10] explored a specific type of shell-and-tube heat exchanger (STHE), where heated water flows through one tube and cold water flows around it. They conducted numerical simulations to model fluid flow and heat transfer, comparing the simulated results with experimental data for validation. Their analysis showed discrepancies between the experimentally measured temperatures and those predicted using ANSYS 13.0.

Irshad et al. [11] compared various STHEs featuring segmental baffles using ANSYS software, aiming to develop and explore the flow and temperatures within the shell and tubes for different baffle assemblies and orientations. Menni et al. [12] employed computational simulations to enhance the thermal behaviour of shell-and-tube heat exchangers by incorporating W-shaped Baffle-type Vortex Generators. Biçer et al. [13] utilized the Taguchi technique after determining various design parameters for a specific baffle type to identify optimal design configurations for optimal performance. Feng et al. [14] investigated a STHE for organic fluid vaporization, highlighting the potential improvement in overall performance by

selecting appropriate working fluid, heated water mass flow rate, and total tube number. The analysis demonstrates that the complex function sacrifices some heat transfer performance while significantly enhancing fluid flow performance, leading to a noticeable reduction in the overall complex function. Among the seven working fluids considered, R152a exhibits the lowest complex function, whereas R236fa shows the highest complex function. Arani and Moradi [15] investigated the enhancement of fluid flow and heat transfer in a segmental baffle shell-and-tube heat exchanger (SBSTHE) by integrating a baffle design with longitudinally ribbed tubes. Their study revealed that a disk baffle shell-and-tube heat exchanger with longitudinal triangular ribbed tubes (DB-TR) outperforms conventional baffle designs, achieving a 39% improvement. Additionally, the combined segmental-disk baffle shell-and-tube heat exchanger with longitudinal triangular ribbed tubes (CSDB-TR) showed a 37% increase in performance, while the configuration with longitudinal circular ribbed tubes (CSDB-CR) resulted in a 13% enhancement.

Marzouk et al. [16] explored the use of bubbles injected with inserts within tubes to enhance thermal performance in shell-and-tube heat exchangers. Their study involved pumping air into tube sides containing wiring nails-circular rod insertion (WNCR) in a straightforward manner, with a constant water tube side flow rate. Marzouk and colleagues [16] have recently drawn considerable interest to the application of bubbles injected with inserts within tubes as a method to improve the thermal efficiency of Shell-and-Tube Heat Exchangers (STHEs). In their specific investigation, air was introduced into the tube sides featuring circular rod insertions composed of wiring nails (WNCR) in a direct manner. The flow rate on the water tube side (TSFR) was adjusted within the range of 14 to 18 Liters per minute (LPM), while the water flow rate on the shell side remained consistently maintained at a suitable level of 18 LPM. In a separate investigation, Safarian et al. [17] employed a shell-and-tube exchanger with a 25% baffle reduction. The study focused on exploring the impact of tube location on heat transfer. The findings indicated that tubes positioned around the shell perimeter had a more significant influence on heat transmission compared to tubes located at the centre of the shell. These selected studies collectively form the foundation for the present research, guiding the exploration of convective heat transfer enhancement through the comprehensive study of flow divider inserts. By building upon and synthesizing insights from these works, the current investigation aims to contribute novel perspectives and practical implications for the advancement of thermal management technologies. The different researcher [17-22] has tried to find some other techniques of enhancing convective heat transfer like using nano fluid. Kale and Gawade [22] has mentioned various methods of heat transfer augmentation for various range of Reynolds number. Various heat transfer augmentation method can also be used to improve efficiency of solar panels [23].

Singh et al. [24] explored the use of aluminium helically corrugated twisted tape inserts to enhance heat transfer in turbulent flow. Their study evaluated the thermal performance, abrasion characteristics, and heat transfer enhancement of a helically fluted duct. They analysed nine spirally corrugated ducts with varying rib-to-width ratios (0.26, 0.17, and 0.22) and rib-height to width ratios (0.06, 0.02, and 0.04). Yadav et al. [25] examined the performance improvement of a solar air heater with rib roughening. The findings revealed that the rib with a shorter pitch achieved the highest Nusselt number at the highest Reynolds number. Additionally, it was observed that this rib with a shorter pitch resulted in the highest friction factor at the lowest Reynolds number.

Liaw et al. [26] investigated convective heat transfer in helical twisted multilobe tubes. Hussen et al. [27] explored the enhancement of heat transfer by employing twisted tape in both horizontal and inclined tubes. They compared the thermal performance of plain tubes and those with twisted tape inserts, finding a strong correlation between experimental and numerical results, with a maximum deviation of 10%. Chandrashekaraiah et al. [28] have worked on the heat transfer enhancement in solar systems. Currently the literature review is not available on the sporadic bisectional inserts, where as the non continious/intermittent twisted tape research is available. sporadic bisectional inserts shows better results compare to the non – continios twisted tape, that is the overall optimal performance was noted, with $\psi$ increasing by 23% and $\eta$ by 55% compared to the plain tube [28-34].

A perforated conical baffle plate with rectangular air deflectors of different inclination angles was used by Md. Atiqur Rahman et al. [35], experimented at Reynolds number ranged between 93,500 and 160,500. Their findings demonstrate that both the inclination angle and the pitch ratio significantly influence the Nusselt number, with the pitch ratio having a more pronounced effect on the friction factor. In a numerical study conducted by Attou et al. [36], the impact of V-shaped grooves on the outer walls of a rotary kiln was analyzed in terms of turbulent flow and heat transfer enhancement. The results showed that increasing the groove depth reduces the outer wall temperature of the rotary kiln compared to smooth walls and results in the highest Nusselt number, particularly for groove depths with h/D ratios of 0.3 and 0.4. Additionally, Raval et al. [37] and Raja et al. [38] have reviewed various techniques for enhancing heat transfer in solar collectors.

Various studies reviewed indicate that inserts enhance heat transfer by disrupting the fluid's boundary layer. However, the presence of inserts also causes area blockage, which increases the friction factor and consequently requires more pumping power. Presently, there exists considerable research focusing on inserts, particularly

exploring different configurations of twisted tape. Some researchers have also investigated flow divider-type inserts, although literature specifically addressing non-continuous types, such as sporadic flow divider inserts, remains scarce. This study aims to bridge this gap by exploring non-continuous flow divider inserts. The hypothesis predicts that the sporadic inserts reduce the blocking of the section and hence the pumping power required will be less. Due to sporadic inserts the pumping power required will be reduced and hence it will help for the increasing Overall performance criteria ($\eta$)

In the current research work Overall Performance Criteria ($\eta$) were calculated at various space ratios. The results showed a moderate improvement, with the highest $\eta$ occurring at a space ratio of 0.59, which corresponds to a 0.015m space between the inserts. For this space ratio, $\eta$ values for different twist angles were as follows: 1.12 to 1.80 for 90°, 1.12 to 1.35 for 60°, 1.15 to 2.22 for 45°, and 1.05 to 1.21 for 30°. The most effective performance was achieved with a twist angle of 45° and a space ratio of 0.59. At this combination, the overall optimal performance was noted, with $\psi$ increasing by 23% and η by 55% compared to the plain tube.

The current research aims to study the effect of various geometric parameters on the working fluid, specifically air, including aspects such as heat transfer, friction factor, thermal enhancement factor, and overall enhancement criteria. Current research is not considering any study related to heat transfer from the insert surface.

In the present study, an experimental setup was developed and tested, evaluating both continuous and sporadic inserts. Conclusions were drawn by plotting graphs of performance parameters such as Nusselt number (*Nu*), friction factor (*f*), highest Thermal Enhancement Factor ($\psi$), and Overall Performance Criteria ($\eta$) against the Reynolds number (*Re*).

The current research can be used in a wide range of industrial and engineering applications where efficient thermal management is essential. This method of heat transfer enhancement can significantly improve the efficiency of thermal energy exchange, leading to reduced energy consumption and operational costs. Additionally, in the field of renewable energy, particularly in solar thermal systems, maximizing convective heat transfer enhances the overall system efficiency, contributing to more sustainable energy solutions.

## THEORY

Figure 1 presents schematic diagram outlining the methodology and experimental configuration employed in this study. The experimental setup centers around a mild steel pipe with an internal diameter of 26 mm, facilitating smooth airflow. A robust 2 hp blower propels air through the pipe, featuring strategically positioned flow control valves at the blower outlet for precise airflow regulation. At the blower outlet termination, an acrylic venturi meter is placed alongside a U-tube manometer designed to measure critical parameters, including head, discharge, and air velocity.

Within the test section, an identical mild steel pipe facilitates airflow. Heat is introduced to the test section through a carefully controlled 1000 Watt heating coil, offering flexibility in heat supply adjustment via a dedicated regulator. This dynamic heating mechanism enables the measured transfer of heat from the inner side of the pipe to the flowing air, a process meticulously monitored and recorded. To minimize heat loss to the atmosphere, the test section pipe is insulated with ceramic wool and further protected by a layer of plastic foam.

Comprehensive thermal profiling of the air is accomplished by strategically placing 12 thermocouples. Each thermocouple contributes to temperature readings displayed on a dedicated temperature indicator board featuring a 7-segment display. Among these readings, $T_1$ indicates the air inlet temperature at the test section, while T10 represents the air outlet temperature at the same section. Intermediate temperatures, denoted as $T_2$ to $T_9$, provide a detailed account of the thermal characteristics of the air along the test section. Utilizing these precise temperature measurements, the heat transfer rate from the heated pipe to the air is accurately computed.

The experimental sequence begins by calculating air flow through an empty pipe. Subsequent iterations introduce carbon fiber inserts, each measuring 25mm x 25mm and 3mm thick, positioned at various angles within the pipe. The resulting heat transfer rates are meticulously determined and subjected to a comparative analysis, yielding valuable insights into the impact of carbon fiber inserts on convective heat transfer (Fig. 2).

The flow divider inserts are fabricated utilizing carbon fiber sheets with a thickness of 3 mm. The process initiates with the cutting of carbon fiber sheets to the designated pitch size and width length, achieved through a shearing machine. Following this, a drilling machine is utilized to generate holes to accommodate the central rod. Please refer to the Figure 3, 4, 5 and 6 for the arrangement of the flow divider type inserts.

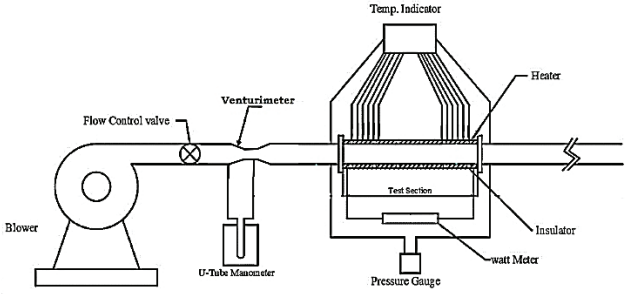


**Figure 1.** Schematic diagram of experimental setup.

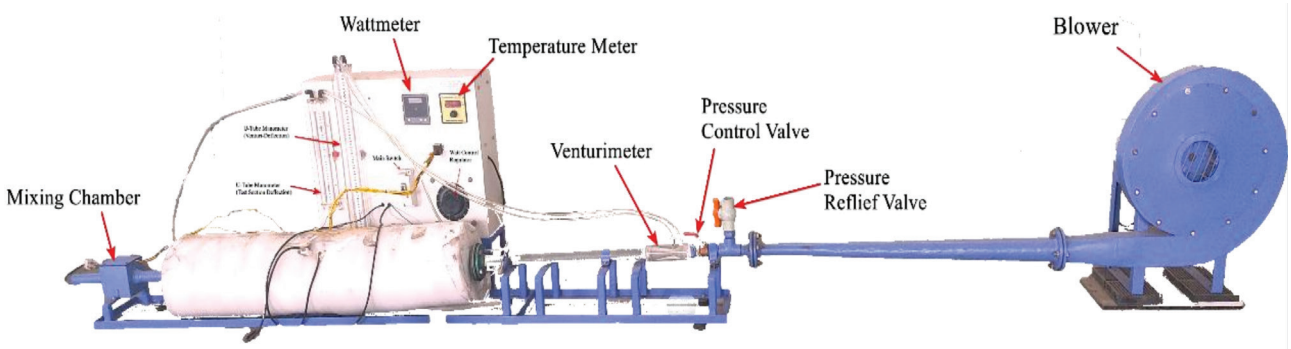


**Figure 2.** Photograph of experimental setup.

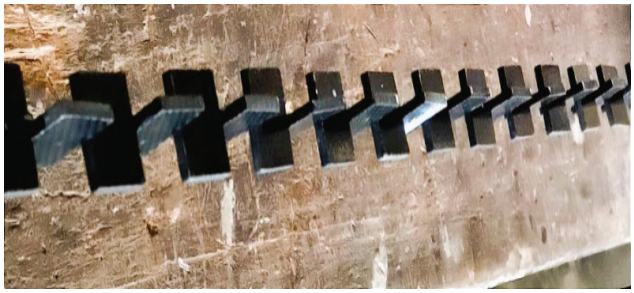

**Figure 3.** Continuous insert at 90° twist angle.

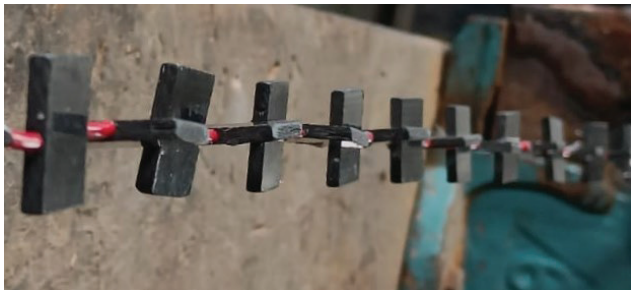

**Figure 4.** Sporadic insert with space S at 90° angle.

**Figure 5.** Locating inserts in the test section.

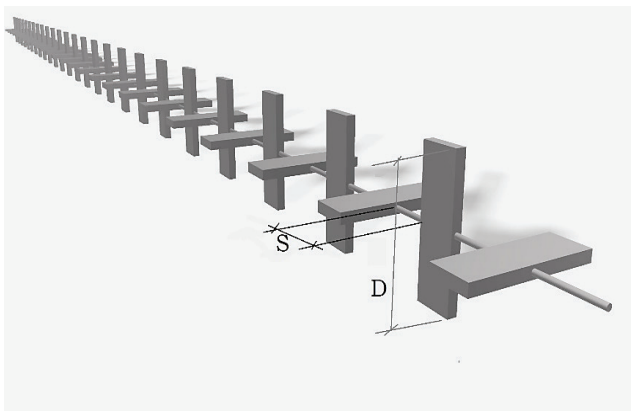


**Figure 6.** Non continuous insert at space ratio of S/D.

**Performance Parameters**

Following are the performance parameters which determines the performance of the system. Various equations of Fluid Mechanics and Heat Transfer is used for performance evaluation. Equation no 1, is taken form book of White and Xue [33], the equation 2, 3, 4 are taken form the book of Incropera et al. [34], the equation no 5 and 6 is taken from the research paper Nalavade et al. [32].

The Reynolds number for the air flow in the test-section is defined as

$$Re = \frac{\rho u D}{\mu} \quad (1)$$

where $u$ is the mean velocity of air in the tube. $\rho$ is density of air in kg/m$^3$, $D$ is diameter of test section pipe in m, $\mu$ is dynamic viscosity in Pa-s.

The total heat transferred to air is estimated by

$$Q = \dot{m} C_P (T_o - T_i) \quad (2)$$

where $T_i$ and $T_0$ is inlet and exit temperature of air, across the test-section. $\dot{m}$ is mass flow rate of air in kg/sec, $C_p$ is specific heat of air in kJ/kgK.

The heat transfer coefficient is given by

$$Q = h\,A_s(T_w - T_{mb}) \tag{3}$$

where $A_s$ denotes the surface area of the tube test-section, $h$ represents the average convective heat transfer coefficient, *Tw* is the average temperature of the tube wall surface, and $T_{mb}$ is the mean bulk fluid temperature obtained through the averaging of air entrance and exit temperatures.

Space ratio (*S*/*D*) is defined as the ratio of Space between two blades of insert (*S*) to the Diameter of the Pipe (*D*)

The influence of heat transfer and fluid flow is respectively demonstrated through the Nusselt number (Nu) and the friction factor (f), elucidating the relationship between them.

$$Nu = \frac{hD}{k} \tag{4}$$

Where Nu is Nusselt number, h is heat transfer coefficient in W/m$^2$.k, D is the diameter of the pipe in m, k is the thermal conductivity of working fluid in W/m.k

$$f = \frac{\Delta P}{\left(\frac{1}{2}\right)\rho u^2\left(\frac{1}{d}\right)} \tag{5}$$

where ΔP is the pressure drop across the test section length in Pa, k is thermal conductivity in *W/mk* , Thermal Enhancement factor ($\psi$) is defined as; $\psi = \frac{h}{h_0}$

Where $h$ = Corvective heat transer coefficient for plain tube fitted with flow divider type insert ($W/m^2K$) and, $h_0$ = Convective heat transfer coefficient for plain tube ($W/m^2K$). Plain tube is tube without any insert or empty tube.

Performance Evaluation Criteria ($\eta$): The evaluation of performance criteria (η) is defined as the ratio of the Nusselt number ratio $\left(\frac{Nu}{Nuo}\right)$ to the friction factor ratio $\left(\frac{f}{fo}\right)^{1/3}$ at the same blower power.

$$\eta = \frac{\left(\frac{Nu}{Nu_0}\right)}{\left(\frac{f}{f_0}\right)^{\frac{1}{3}}} \tag{6}$$

## RESULTS AND DISCUSSION

The experimental results are analyzed using various graphical representations, with different observational parameters recorded at varying Reynolds numbers. The study investigates the effect of changing the twist angle of a flow divider-type insert on convective heat transfer. The findings indicate that increasing the Reynolds number leads to a higher convective heat transfer rate, due to the increased flow rate that enhances turbulence. Figure 7 demonstrates the effect of altering the twist angle on the Nusselt number.

As the twist angle decreases, the size of the fluid pockets also decreases, which in turn intensifies turbulence. This reduction in twist angle correlates with an increase in the Nusselt number. The highest Nusselt number is observed at a 45° twist angle, where the average Nusselt number is 2.21 times higher than that of a plain tube.

Experimental data were collected using different twist angles—specifically 90°, 60°, 45°, and 30°—across Reynolds numbers ranging from 7000 to 21000. Predicted correlations are valid for the Re ranges from 7000 to 12000. To evaluate the effect of spacing between the inserts (sporadic insert), results were obtained for different space ratios (0.19, 0.39, 0.59, 0.78) combined with various twist angles. The data was analyzed by plotting various graphs, with result parameters such as Nusselt number, friction factor, thermal enhancement factor, and performance evaluation criteria plotted against Reynolds number to draw conclusions and observe trends.

The graph is constructed for four twist angles: 90°, 60°, 45°, and 30°. Correspondingly, there are four distinct lines on the graph. Analysis of the graph reveals that the Nusselt number is dependent on the Reynolds number. The 45° twist angle yields the highest Nusselt number.

The trend line equation for the 45° twist angle is determined to be-

$$\text{Nu} = 6.2129\text{Re} + 61.918 \tag{7}$$

The equations vary for different angles: for a 60° twist angle, the equation is

$$\text{Nu} = 6.5662\text{Re} + 41.026 \tag{8}$$

for a 30° twist angle, the equation is

$$\text{Nu} = 5.217\text{Re} + 42.535 \tag{9}$$

for a 90° twist angle the equation is

$$\text{Nu} = 5.0007\text{Re} + 35.649 \tag{10}$$

and for a plain tube, the equation is

$$\text{Nu} = 5.003\text{Re} + 17.993 \tag{11}$$

The influence of changing the cyclic angle of twist of the flow divider type insert on the friction factor is depicted in Figure 8. Remarkably, the pressure drops for the tube equipped with the flow divider type insert is noted to rise as the cyclic angle of twist decreases, indicating a consistent trend in the friction factor. Figures 8 and 9 collectively depict the impacts of varying the cyclic angle of twist of the flow divider type insert on the friction factor and friction factor ratio, respectively.

Specifically, the friction factor is found to vary from 0.10 to 0.07 for a 90° angle, from 0.28 to 0.18 for a 60° angle,

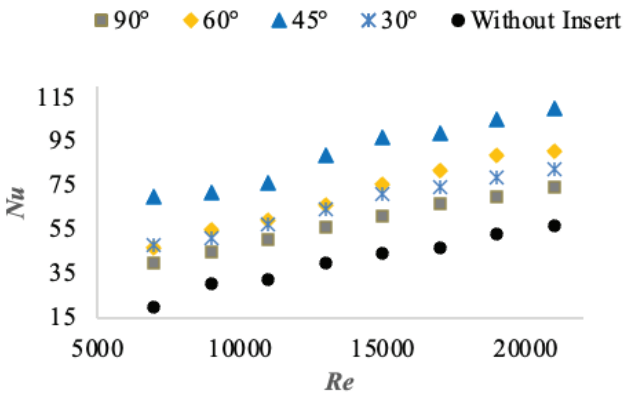


**Figure 7.** Influence of change in the angle of twist of flow divider type insert on Nusselt number.

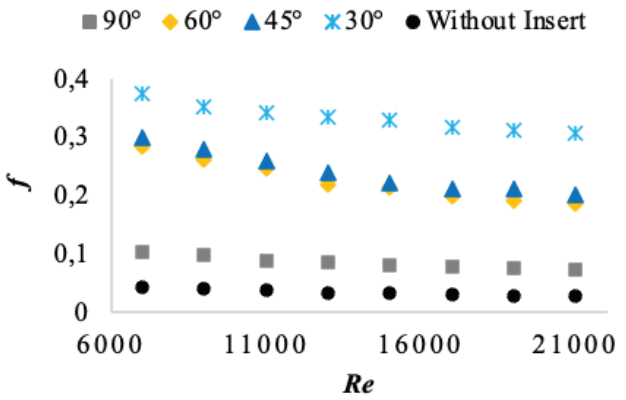


**Figure 8.** Influence of change in the angle of twist of flow divider type insert on friction factor.

from 0.30 to 0.20 for a 45° angle, and from 0.37 to 0.30 for a 30° angle. Average friction factor of 45° angle is 7 times more than the average friction factor of plain tube. This is because of blocking of the flow of air by the insert.

The illustration in Figure 10 depicts the impact of adjusting the angle of twist of the flow divider type insert on the thermal enhancement factor ($\psi$). It is evident that a decrease in the angle of twist from 90° to 60°, 45°, and 30° corresponds to an increase in the thermal enhancement factor. The findings indicate that as the angle of twist decreases from 90° to 30° in incremental steps, the thermal enhancement factor increases by 1.28 to 1.43 times for a 90° angle, 1.38 to 1.65 for a 60° angle, 1.39 to 1.72 for a 45° angle, and 1.48 to 2.13 for a 30° angle, in comparison to a plain tube without an insert.

As a result, it is noted that the maximum enhancement in heat transfer occurs when the tube incorporates the flow divider type insert with an angle of twist equal to 45°. Average thermal enhancement factor at 45° is 1.7 times more than that of plain tube.

A parameter the 'space ratio' is introduced, defined as the ratio of the space between the inserts to the diameter of the tube. The spacing between the inserts is adjusted to 0.005m, 0.010m, 0.015m, and 0.020m., resulting in space ratios of 0.19, 0.39, 0.59, and 0.78, respectively.

Figure 11 depicts the impact of varying the space ratio on the Thermal Enhancement Factor ($\psi$) at a twist angle of 90°. Similar observations reveal an improvement in the Thermal Enhancement Factor due to the presence of space between the inserts. Remarkably, a space ratio of 0.59 yields superior results, with the highest Thermal Enhancement Factor reaching 1.8 at a Reynolds number of 7000. The average thermal enhancement factor ($\psi$) at

59 space ratio and 90° twist angle is maximum and it is 21% more than that of continuous blade insert.

Figure 12 illustrates the impact of altering the space ratio on the Thermal Enhancement Factor ($\psi$) at a twist angle of 60°. Similar observations indicate an enhancement in the Thermal Enhancement Factor due to the presence of space between the inserts. Notably, a space ratio of 0.59 yields superior results, with the highest Thermal Enhancement

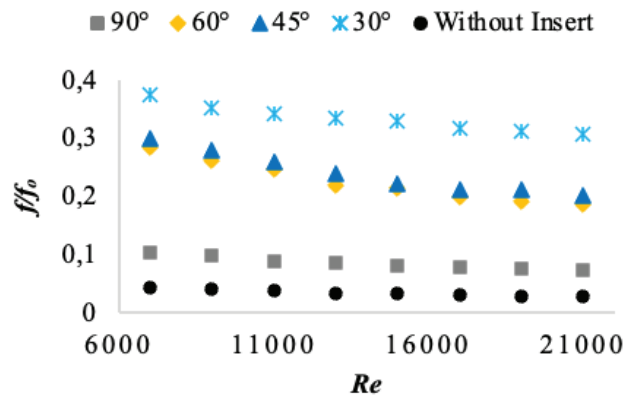


**Figure 9.** Influence of change in the cyclic angle of twist of flow divider type insert on friction factor ratio ($f/f_o$).

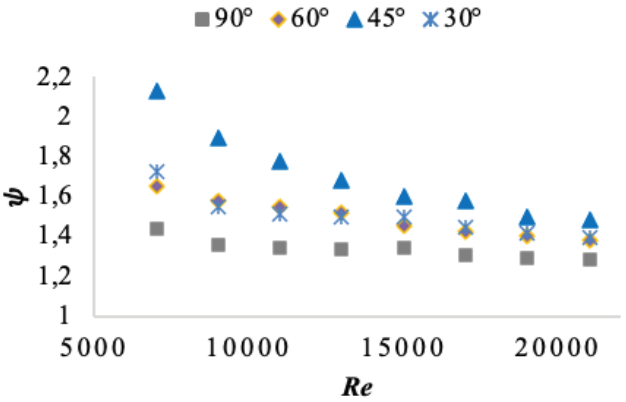


**Figure 10.** Influence of change in the cyclic angle of twist of flow divider type insert on Thermal Enhancement Factor.

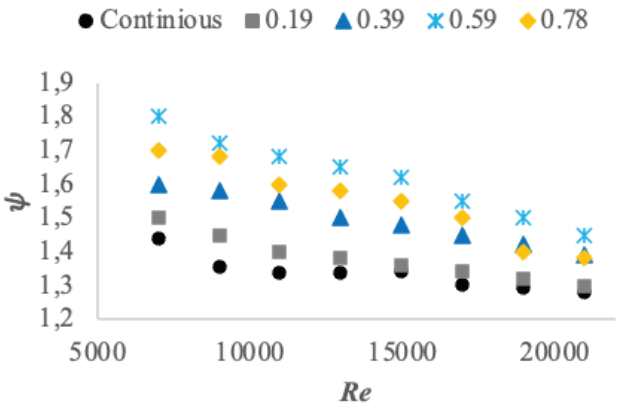


**Figure 11.** Influence of change of space ratio on Thermal Enhancement Factor ($\psi$) at angle of twist 90°.

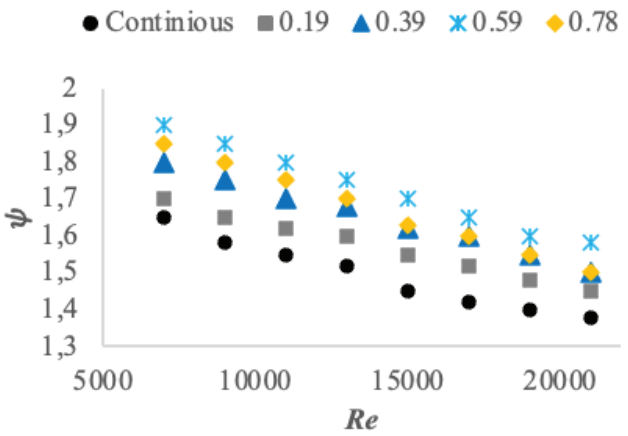


**Figure 12.** Influence of change of space ratio on Thermal Enhancement Factor at angle of twist 60°.

Factor reaching 1.85 at a Reynolds number of 7000. The average thermal enhancement factor ($\psi$) at 0.59 space ratio and at 60° twist angle is maximum and it is 15% more than that of continuous blade insert.

Figure 13 illustrates the impact of altering the space ratio on the Thermal Enhancement Factor ($\psi$) at a twist angle of 45°. The graph indicates that a space ratio of 0.59 yields superior results compared to other space ratios. The highest Thermal Enhancement Factor achieved is 2.4 at a Reynolds number of 7000. The average thermal enhancement factor ($\psi$) at 0.59 space ratio and at 45° twist angle is maximum and it is 15% more than that of continuous blade insert.

Figure 13 shows that the Nusselt number (Nu) is a function of the Reynolds number (Re) and the space ratio. The trend line equations derived from the graph illustrate this relationship. For a space ratio of 0.19, the equation is-

$$Nu = -0.00004Re + 2.3029. \quad (12)$$

For a space ratio of 0.39, the equation becomes,

$$Nu = -0.00003Re + 2.1963 \quad (13)$$

For a space ratio of 0.59, the equation is,

$$Nu = -0.00005Re + 2.6113, \quad (14)$$

For a space ratio of 0.78, the equation is

$$Nu = -0.00004Re + 2.3074. \quad (15)$$

Figure 14 illustrates the impact of altering the space ratio on the Thermal Enhancement Factor ($\psi$) at a twist angle of 30°. Similar to the observations in the previous analysis, the Thermal Enhancement Factor is enhanced due to the presence of space between the inserts. Notably, a space ratio of 0.5905 yields superior results, with the highest Thermal Enhancement Factor reaching 2.2 at a Reynolds number of 7000. The average thermal enhancement factor ($\psi$) at 0.59 space ratio and at 30° twist angle is maximum and it is 14% more than that of continuous blade insert.

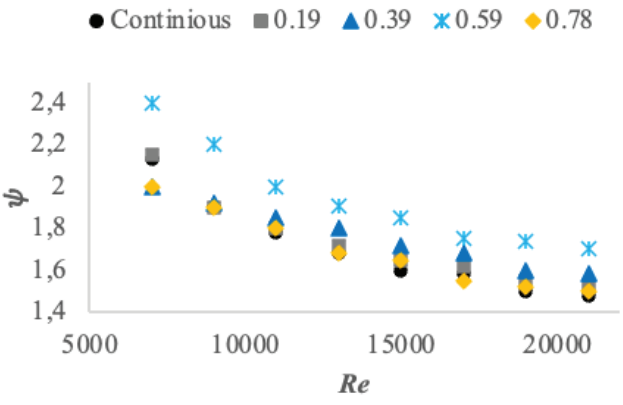


**Figure 13.** Influence of change of space ratio on Thermal Enhancement Factor at angle of twist 45°.

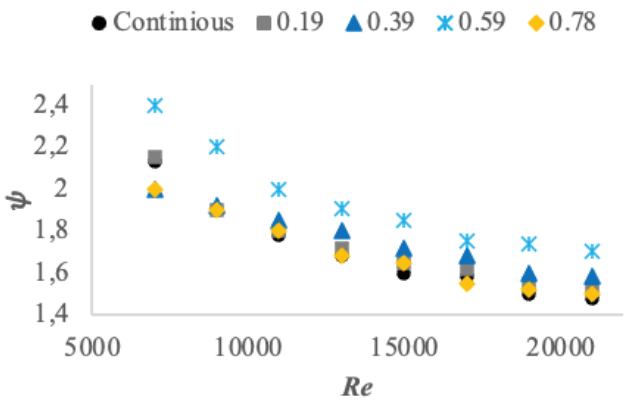


**Figure 14.** Influence of change of space ratio on Thermal Enhancement Factor at angle of twist 30°.

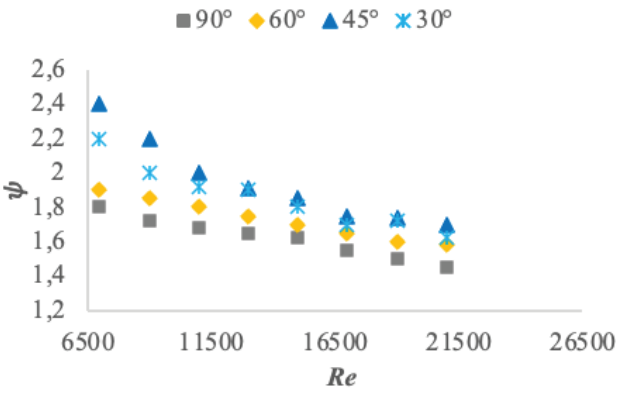


**Figure 15.** Influence of change of various angle of twist on Thermal Enhancement Factor.

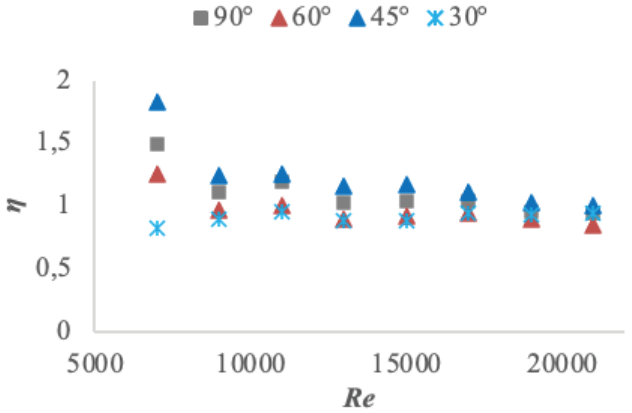


**Figure 16.** Influence of change of twist angle on Performance Evaluation Criteria.

Based on the collected readings across various space ratios, it is noted that the Thermal Enhancement Factor ($\psi$) attains its maximum value at a space ratio of 0.59 for all twist angles. As depicted in Figure 15, the impact of altering the space ratio on the Thermal Enhancement Factor at different angles of twist is showcased. Specifically, at a space ratio of 0.59, a twist angle of 45° yields the highest Thermal Enhancement Factor, reaching 2.4. The average thermal enhancement factor ($\psi$) at 0.59 space ratio is maximum and it is 23% more than that of continuous blade insert.

Figure 16 illustrates the impact of varying the angle of twist of the novel flow divider type insert on the Performance Evaluation Criterion ($\eta$) with continuous inserts. It is noted that the insert with a 45° angle of twist outperforms inserts with other twist angles. The $\eta$ values range from 1.006 to 1.831 for the flow divider type insert with a 45° angle of twist. The maximum Performance Evaluation Criteria ($\eta$) is observed for 45° twist angle and it is 22% more than the plain tube.

Figure 17 illustrates the impact of altering the space ratio at a 90° angle of twist on the Performance Evaluation Criterion ($\eta$). It is observed that as the Reynolds Number increases, the $\eta$ decreases. Notably, a space ratio of 0.5905 exhibits superior performance compared to other space ratios. For a space ratio of 0.5905, the $\eta$ ranges from 1.123 to 1.801. The maximum Performance Evaluation Criteria ($\eta$) is observed for 0.59 space ratio and at 90° twist angle and it is 32% more than continuous insert.

Figure 18 illustrates the impact of varying the space ratio at a 60° angle of twist on the Performance Evaluation

Criterion ($\eta$). The trend shows that with an increase in the Reynolds Number, the $\eta$ decreases. Notably, a space ratio of 0.59 demonstrates superior performance compared to other space ratios. Specifically, for a space ratio of 0.59, the $\eta$ ranges from 1.123 to 1.352. The maximum Performance Evaluation Criteria ($\eta$) is observed for 0.59 space ratio and at 60° twist angle and it is 17% more than continuous insert.

Figure 19 illustrates the impact of altering the space ratio at a 45° angle of twist on the Performance Evaluation Criterion ($\eta$). It is observed that as the Reynolds Number increases, the $\eta$ experiences a decrease. Significantly, a space ratio of 0.59 demonstrates superior performance

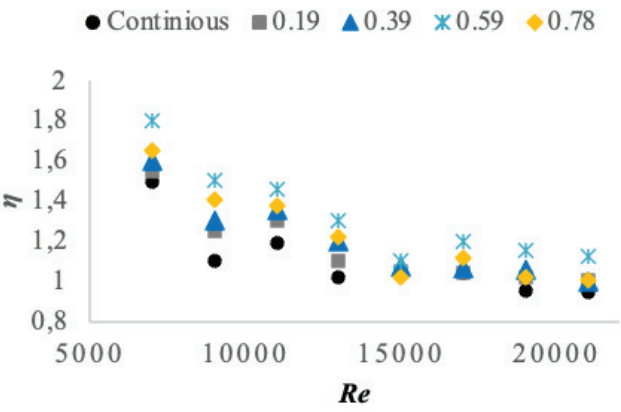


**Figure 17.** Influence of change of space ratio on Performance evaluation Criteria at 90° twist angle.

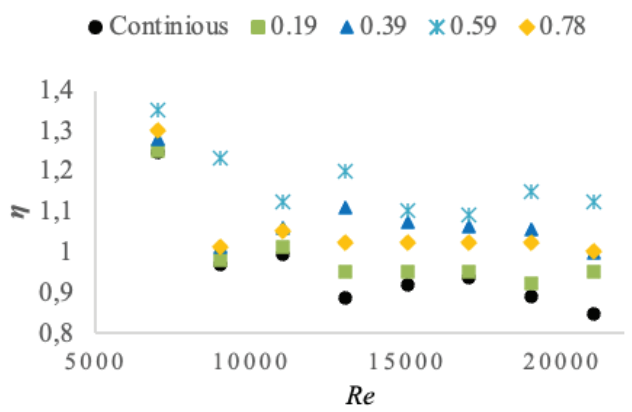


**Figure 18.** Influence of change of space ratio on Performance evaluation Criteria at 60° twist angle.

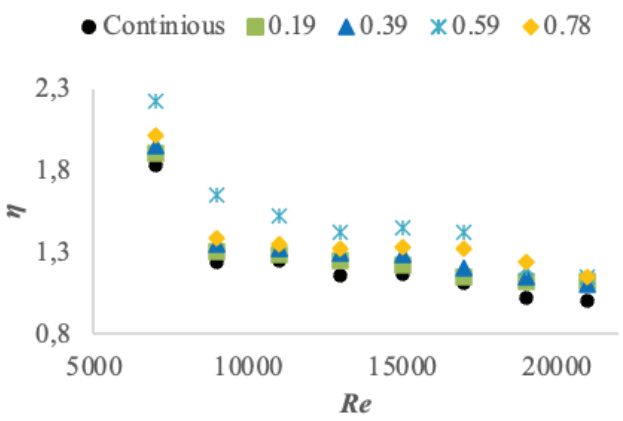


**Figure 19.** Influence of change of space ratio on Performance evaluation Criteria at 45° twist angle.

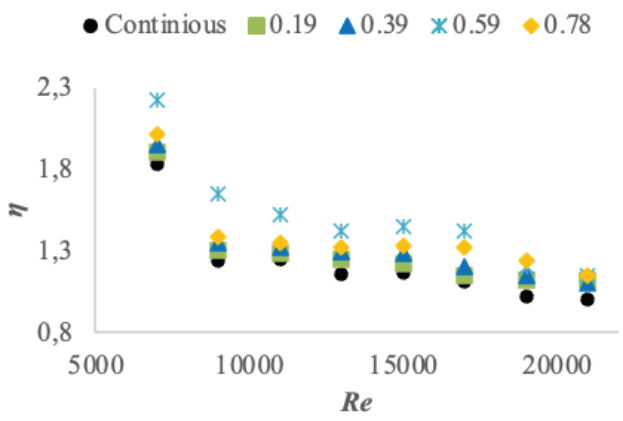


**Figure 20.** Influence of change of space ratio on Performance evaluation Criteria at 30° twist angle.

compared to other space ratios. Specifically, for a space ratio of 0.59, the $\eta$ ranges from 1.152 to 2.223. The maximum Performance Evaluation Criteria ($\eta$) is observed for 0.59 space ratio and at 45° twist angle it is 22% more than continuous insert.

Figure 20 illustrates the impact of varying the space ratio at a 30° angle of twist on the Performance Evaluation Criterion ($\eta$). The trend indicates that with an increase in the Reynolds Number, the $\eta$ undergoes a decrease. Notably, a space ratio of 0.59 demonstrates superior performance in comparison to other space ratios. Specifically, for a space ratio of 0.59, the $\eta$ ranges from 1.051 to 1.11. The maximum Performance Evaluation Criteria ($\eta$) is observed for 0.59 space ratio and at 30° twist angle and it is 15% more than continuous insert.

Figure 21 illustrates the impact of altering the space ratio at various angles of twist on the Performance Evaluation Criterion ($\eta$) with a fixed space ratio of 0.59. The trend indicates that as the Reynolds Number increases, the $\eta$ experiences a decrease. Notably, a twist angle of 45° demonstrates superior performance compared to other twist angles. Specifically, for a 45° angle and a space ratio of 0.5905, the $\eta$ ranges from 1.152 to 2.223. The maximum Performance Evaluation Criteria ($\eta$) is observed for 45° twist angle for space ratio of 0.59 and it is 55% more than that of plain tube. To understand the simultaneous effects of twist angle, Reynolds number (*Re*), and space ratio on the overall enhancement factor ($\eta$), a series of experiments were conducted. Refer Figure 22.

Overall Enhancement Factor ($\eta$) was plotted at a 45° twist angle and a space ratio of 0.59. Initially, the twist angle was optimized by plotting the Nusselt number (*Re*), Thermal Enhancement Factor, and Overall Enhancement Factor ($\eta$) against the Reynolds number (*Re*). The highest performance was observed at a 45° twist angle.

Following the optimization of the twist angle, the performance parameters were examined at various space ratios of 0.19, 0.39, 0.59, and 0.78. The maximum performance was recorded at a space ratio of 0.59. To analyze the combined influence of these parameters, graphs were plotted

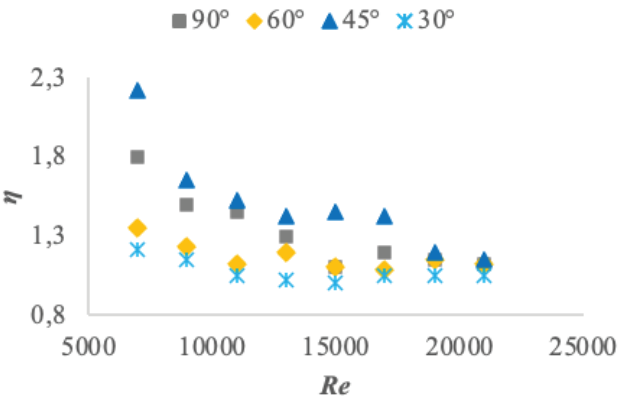


**Figure 21.** Influence of change of twist angle on Performance evaluation Criteria at space ratio 0.59.

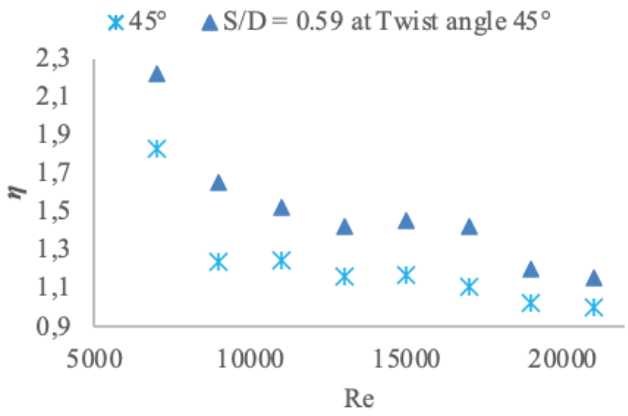


**Figure 22.** Simultaneous effect of Twist angle and Space ratio, (Graph at Optimum twist angle 45° and Space ratio 0.59).

across a range of Reynolds numbers (*Re*) against the Overall Performance Parameter ($\eta$).

The equations of the trend lines for the $\eta$ are provided below:

For a 45° twist angle with continuous insert:

$$\eta = -6\times10^{-5}\,\mathrm{Re}+2.3418 \quad (16)$$

For a space ratio of 0.59 and a 45° twist angle:

$$\eta = -4\times10^{-5}\,\mathrm{Re}+1.8321 \quad (17)$$

It was observed that both performance and heat transfer were more efficient at lower Reynolds numbers, specifically in the range of 7000 to 15000. Beyond this range, a sudden drop in heat transfer was noted. Thus, for optimal performance, it is recommended to maintain a 45° twist angle and a space ratio of 0.59 at Reynolds numbers between 7000 and 15000.

## CONCLUSION

In this research, an experimental investigation was conducted to study the fluid flow and heat transfer characteristics of a circular tube fitted with a sporadic flow divider type turbulator under turbulent flow conditions. The study focused on the performance of heat exchanger tubes equipped with flow dividers with space to diameter ratios (S/D) of 0.19, 0.39, 0.59, and 0.78. The results indicate that the flow divider turbulator effectively disrupts the boundary layer, thereby enhancing thermal performance. However, the solid flow divider also partially obstructs the test section, leading to increased friction and pumping power. Future studies could explore the use of flow dividers with specific porosities to optimize heat transfer efficiency and reduce friction. The key findings from this experimental study are as follows:

1) Flow divider inserts with twist angles of 90°, 60°, 45°, and 30° were tested. As the twist angle decreases, fluid flow blockage increases, which enhances fluid mixing from the core to the tube wall and improves convective heat transfer. The corresponding Nusselt numbers range from 40.12 to 74.45 for a 90° twist, 46.95 to 90.56 for a 60° twist, 70.12 to 110.12 for a 45° twist, and 47.97 to 82.9 for a 30° twist.
2) The thermal enhancement factor ($\psi$) shows significant improvement across different twist angles. For a 90° twist, $\psi$ increases by 1.28 to 1.43 times compared to a plain tube; for a 60° twist, $\psi$ increases by 1.38 to 1.65 times; for a 45° twist, $\psi$ rises by 1.48 to 2.13 times; and for a 30° twist, $\psi$ increases by 1.39 to 1.72 times.
3) The highest friction factor is observed at a 30° twist angle, ranging from 0.30 to 0.37, due to the significant flow area blockage.
4) The overall performance criteria ($\eta$) were calculated at different space ratios, with the highest $\eta$ observed at a space ratio of 0.59, corresponding to a 0.015 m space between inserts. For this space ratio, $\eta$ values are 1.12 to 1.80 for a 90° twist, 1.12 to 1.35 for a 60° twist, 1.15 to 2.22 for a 45° twist, and 1.05 to 1.21 for a 30° twist.
5) The optimal performance was achieved with a 45° twist angle and a space ratio of 0.59, resulting in a 23% increase in $\psi$ and a 55% increase in η compared to a plain tube.

These findings suggest that the use of flow divider type turbulators, particularly with optimized twist angles and space ratios, can significantly enhance the thermal and overall performance of heat exchanger tubes under turbulent flow conditions.

## NOMENCLATURE

| | |
|---|---|
| $A$ | Surface area of the experimental test section, measured in square meters ($m^2$). |
| $Cp$ | Specific heat of air at constant pressure, expressed in joules per kelvin (J/k). |
| $D$ | Inner diameter of the plain tube, measured in meters (m). |
| $f$ | Friction factor, a dimensionless number. |
| $h$ | Average convective heat transfer coefficient ($W/m^2.k$). |
| $k$ | Thermal Conductivity (W/m·K) - Ability of a material to conduct heat, in watts per meter-kelvin. |
| $L$ | Length of the test section, expressed in meters (m). |
| $\dot{m}$ | Mass Flow Rate(kg/s) - Amount of mass flowing per unit time, in kilograms per second) |
| $Nu$ | Nusselt number, a dimensionless quantity. |
| $P$ | Insert pitch, measured in meters (m). |
| $P_r$ | Prandtl number, a dimensionless quantity. |
| $Q$ | Heat transfer rate, measured in watts (W). |
| $R_e$ | Reynolds number, a dimensionless quantity. |
| $S$ | Space between the two blades of the insert, in meters (m). |
| $T_i$ | Initial temperature of the fluid, in degrees Celsius (°C). |
| $T_0$ | Iinal temperature of the fluid, in degrees Celsius (°C). |
| $T_w$ | Temperature of the wall surface, in degrees Celsius (°C). |
| $T_{mb}$ | Average temperature of the bulk fluid, in degrees Celsius (°C). |
| $\dot{v}$ | Volume Flow Rate ($m^3/s$) - Volume of fluid passing through per unit time, in cubic meters per second |

Greek symbols

| | |
|---|---|
| $\rho$ | Density ($kg/m^3$) - Mass per unit volume, measured in kilograms per cubic meter |
| $\mu$ | Dynamic Viscosity ($Ns/m^2$) - Measure of fluid's internal resistance to flow, expressed in Newton-seconds per square meter. |
| $\psi$ | Thermal Enhancement Factor, TEF - Dimensionless factor representing thermal enhancement. |
| $\eta$ | Performance Evaluation Criteria - Criteria used for performance evaluation. |

Subscripts

| | |
|---|---|
| $i$ | Inlet |
| $o$ | Outlet |
| $bm$ | Bulk mean |
| $0$ | Plain tube |
| $s$ | Surface |

## ACKNOWLEDGEMENT

The authors sincerely acknowledge the invaluable support and research facilities provided by Nagesh Karajagi Orchid College of Engineering and Technology, Solapur. Their generous assistance and resources played a crucial role in facilitating the successful completion of this research work.

## AUTHORSHIP CONTRIBUTIONS

Authors equally contributed to this work.

## DATA AVAILABILITY STATEMENT

The authors confirm that the data that supports the findings of this study are available within the article. Raw data that support the finding of this study are available from the corresponding author, upon reasonable request.

## CONFLICT OF INTEREST

The author declared no potential conflicts of interest with respect to the research, authorship, and/or publication of this article.

## ETHICS

There are no ethical issues with the publication of this manuscript.

## REFERENCES

[1] Kumar N, Jhinge P. Effect of segmental baffles at different orientation on the performances of single pass shell and tube heat exchanger. Int J Eng Trends Technol 2014;15:423–428. [CrossRef]

[2] Bichkar P, Dandgaval O, Dalvi P, Godase R, Dey T. Study of shell and tube heat exchanger with the effect of types of baffles. Procedia Manuf 2018;20:195–200. [CrossRef]

[3] Ali MK, Naji S. Performance analysis of shell and tube heat exchanger parametric study. Case Stud Therm Eng 2018;12:563–568. [CrossRef]

[4] Joemer CS, Thomas S, Rakesh D, Nidheesh P. Optimization of shell & tube heat exchanger by baffle inclination and baffle cut. Int J Innov Res Sci Eng Technol 2015;4:69–73.

[5] Son Y, Shin J. Performance of a shell and tube heat exchanger with spiral baffles plates. KSME Int J 2001;15:1555–1562. [CrossRef]

[6] Petrik M, Szepesi G. Shell side CFD analysis of a model shell and tube heat exchanger. Chem Eng. 2018;70:313–318.

[7] Edward G, Volker G. Pressure drop on the shell side of shell-and-tube heat exchangers with segmental baffles. Chem Eng Process 1997;36:149–159. [CrossRef]

[8] Gu X, Luo Y, Xiong X, Wang K, Wang Y. Numerical and experimental investigation of the heat exchanger with trapezoidal baffles. Int J Heat Mass Transf 2018;127:598–606. [CrossRef]

[9] Akpbio E, Oboh I, Aluyor E. The effect of baffles in shell and tube heat exchangers. Adv Mater Res 2009;62–64:694–699. [CrossRef]

[10] Singh G, Kumar H. Computational fluid dynamics analysis of shell and tube heat exchanger. J Civ Eng Environ Technol 2014;1:66–70.

[11] Irshad M, Kaushar M, Rajmohan G. Design and CFD analysis of shell and tube heat exchanger. Int J Eng Sci Comput 2017;7:212452909.

[12] Menni Y, Chamkha AJ, Ameur H, Mustafa. Enhancement of the hydrodynamic characteristics in shell-and-tube heat exchangers by using W-baffle vortex generators. Period Polytech Mech Eng 2020;64:212–223. [CrossRef]

[13] Biçer N, Engin T, Yaşar H, Büyükkaya E, Aydın A, Topuz A. Design optimization of a shell-and-tube heat exchanger with novel three-zonal baffle by using CFD and Taguchi method. Int J Therm Sci 2020;155:106417. [CrossRef]

[14] Feng H, Chen L, Wu Z, Xie Z. Constructal design of a shell-and-tube heat exchanger for organic fluid evaporation process. Int J Heat Mass Transf 2019;131:750–756. [CrossRef]

[15] Arani AAA, Moradi R. Shell and tube heat exchanger optimization using new baffle and tube configuration. Appl Therm Eng 2019;157:113736. [CrossRef]

[16] Marzouk SA, Abou Al-Sood MM, ElFakharany MK, El-Said EMS. Thermo-hydraulic study in a shell and tube heat exchanger using rod inserts consisting of wire-nails with air injection: experimental study. Int J Therm Sci 2020;161:106742. [CrossRef]

[17] Safarian MR, Fazelpour F, Sham M. Numerical study of shell and tube heat exchanger with different cross-section tubes and combined tubes. Int J Energy Environ Eng 2019;10:33–46. [CrossRef]

[18] Wildi-Tremblay P, Gosselin L. Minimizing shell-and-tube heat exchanger cost with genetic algorithms and considering maintenance. Int J Energy Res 2007:1272. [CrossRef]

[19] Khan Z, Khan ZA. Experimental and numerical investigations of nano-additives enhanced paraffin in a shell-and-tube heat exchanger: a comparative study. Appl Therm Eng 2018:115436660. [CrossRef]

[20] Fares M, AL-Mayyahi M, AL-Saad M. Heat transfer analysis of a shell and tube heat exchanger operated with graphene nanofluids. Case Stud Therm Eng 2020;18:100584. [CrossRef]

[21] El-Saida EMS, Abou Al-Sood MM. Shell and tube heat exchanger with new segmental baffles configurations: a comparative experimental investigation. Appl Therm Eng 2019;150:039. [CrossRef]

[22] Kale SS, Gawade SS. Heat transfer augmentation in forced convection with regularly spaced inserts—a review. Techno-Societal 2022 Proc 4th Int Conf Adv Technol Societal Appl Vol 2.

[23] Kale SS, Gawade SS, Birajdar BR. Improving conversion efficiency of solar panel by cooling system. Techno-Societal 2022 Proc 4th Int Conf Adv Technol Societal Appl Vol 2.

[24] Singh A, Gupta M, Tiwari DK, Verma RP. Utilization of aluminium helically corrugated twisted tape inserts for heat transfer enhancement of turbulent flow. Mater Today 2023;92:1623–1628. [CrossRef]

[25] Yadav AS, Mishra A, Dwivedi K, Agrawal A, Galphat A, Sharma N. 4th International Conference on Advances in Mechanical Engineering and Nanotechnology. Mater Today 2022;63:726–730. [CrossRef]

[26] Liaw KL, Kurnia JC, Putra ZA, Aziz M, Sasmito AP. Enhanced turbulent convective heat transfer in helical twisted multilobe tubes. Int J Heat Mass Transf 2023;202:123687. [CrossRef]

[27] Hussen HM, Habeeb L, Kadhim ZK. Heat transfer enhancement by using twisted tape in horizontal and an inclined tube. J Mech Eng Res Dev 2020;43:106–124.

[28] Chandrashekaraiah M, Nagappan B, Devarajan Y. Hybrid power generation: experimental investigation of PCM and TEG integration with photovoltaic systems. Int Res J Multidiscip Technovation 2024;6:225–231. [CrossRef]

[29] Arulprakasajothi M, Poyyamozhi N, Saranya A, Elangovan K, Devarajan Y, Murugapoopathi S, Amesho KTT. An experimental investigation on winter heat storage in compact salinity gradient solar ponds with silicon dioxide particulates infused paraffin wax. J Energy Storage 2024;82:110503. [CrossRef]

[30] Jothilingam M, Balakrishnan N, Kannan TK, Devarajan Y. Experimental investigation of a solar still system with a preheater and nanophase change materials. Proc Inst Mech Eng Part E J Process Mech Eng 2024:09544089241247455.

[31] Thulasiram R, Murugapoopathi S, Surendarnath S, Nagappan B, Devarajan Y. RSM-based empirical modeling and thermodynamic analysis of a solar flat plate collector with diverse nanofluids. Process Integr Optim Sustain 2024;8:1–14. [CrossRef]

[32] Nalavade S, Prabhune C, Sane N. Effect of novel flow divider type turbulators on fluid flow and heat transfer. Therm Sci Eng Prog 2018;9:322–331. [CrossRef]

[33] White FM, Xue H. Fluid Mechanics. 9th ed. Tata McGraw-Hill; 2022.

[34] Incropera FP, DeWitt DP, Bergman TL, Lavine AS. Incropera's principles of heat and mass transfer. 8th ed. New York: John Wiley & Sons; 2017.

[35] Rahman MA, Dhiman SK. Thermo-fluid performance of a heat exchanger with a novel perforated flow deflector type conical baffles. J Therm Eng 2024;10:868–879. [CrossRef]

[36] Attou Y, Bouhafs M, Feddal A. Numerical analysis of turbulent flow and heat transfer enhancement using V-shaped grooves mounted on the rotary kiln's outer walls. J Therm Eng 2024;10:350–359. [CrossRef]

[37] Raval P, Ramani B. Heat transfer enhancement techniques using different inserts in absorber tube of parabolic trough solar collector: a review. J Therm Eng 2024;10:1068–1091. [CrossRef]

[38] Raja GA, Natarajan R, Gaikwad PR, Basil E, Borse SD, Sundararaj M. Heat enhancement in solar flat plate collectors—a review. J Therm Eng 2024;10:773–789. [CrossRef]